ADVANCED MATERIALS TECHNOLOGIES
www.advmattechnol.de

Transcribing In Vivo Blood Vessel Networks into In Vitro Perfusable Microfluidic Devices

*Yih Yang Chen, Benjamin R. Kingston, and Warren C. W. Chan**

The 3D architecture of blood vessel networks dictates how nutrients, waste, and drugs are transported. These transport processes are difficult to study in vivo, leading researchers to develop methods to construct vessel networks in vitro. However, existing methods require expensive, customized equipment and cannot create large (>1 cm^3) constructs. This makes them inaccessible to many researchers or educators. Here, a method that transcribes 3D images of blood vessel networks into physical microfluidic devices is developed. The method takes 3D images of blood vessel networks and uses fused-filament 3D fabrication with standard polylactic acid (PLA) filament to print the imaged vessel network. The 3D printout is cast in polydimethylsiloxane (PDMS) and dissolved, producing vessel channels that are lined with endothelial cells. Devices imprinted with different vessel networks including small intestinal villi, pancreatic islets, and tumors from mice and humans are created. The method replicates the complex geometries of blood vessel networks in an in vitro device with commonly available equipment and materials. This increases the accessibility of this technology by allowing researchers or educators without access to expensive laser ablation microscope set-ups or custom 3D printers to be able to create vasculature network devices.

1. Introduction

Blood vessels are a critical component of any healthy, diseased, or engineered tissue. The blood vessel architecture determines how nutrients, waste, and drugs are transported.[1] To study how vascular networks affect disease progression and for engineering vascularized tissues, it is important to engineer in vitro devices that recapitulate the geometry of natural vessel networks. Several methods have been developed to recreate the network of vessels observed in vivo into manufactured microfluidic devices. These methods can be categorized by their method of fabrication, and include coaxial microfluidic spinning,[2–7] micromolding,[8–10] or 3D printing.[11–20] A review of vascular manufacturing technologies by Xie et al. summarizes these technologies.[21] These methods have advantages, but require the use of customized and expensive equipment or materials, including customized laser-ablation microscopes, clean rooms, custom 3D printers, and unique hydrogels or bioinks. For example, laser-ablation has been used to create detailed replicates of the blood vessel networks seen in vivo,[18,19] but requires expensive two-photon microscopes, custom stage controllers, and/or custom software. 3D printing can be used to generate in vivo vascular patterns in devices, but current methods require custom-built 3D printers, which use specialized inks, bioinks, and software.[11,12,14–16] Many researchers and educators do not have access to these technologies, so there is a need for a technique that uses readily available materials to replicate natural blood vessel networks without expensive or complicated manufacturing tools and expertise.

In this project, we developed a simple method termed CLARITY-to-REALITY (C2R) that transcribes 3D images of blood vessel networks into perfusable microfluidic devices using a basic commercial 3D printer and common materials. The goal of these devices is to provide a platform to study drug, nutrient or waste interaction with endothelial cells under flow conditions within a vessel network that replicates the in vivo vessel network. We use an automated script to convert 3D fluorescent microscopy images of vessel networks into stereolithography files (.stl), which are used in most commercial 3D printers. We 3D print the vessel model using a commercially available fused filament 3D printer, freely available 3D printing software, and inexpensive polylactic acid (PLA) filament. The 3D printed model is cast in polydimethylsiloxane (PDMS) and dissolved to create a microfluidic device that is imprinted with the imaged 3D vessel network. We also developed a method for lining the large and complex vessel networks with endothelial cells. This results in a living, in vitro 3D vessel network. Our method can

Y. Y. Chen, B. R. Kingston, Prof. W. C. W. Chan
Institute of Biomaterials and Biomedical Engineering
University of Toronto
Toronto, Ontario M5S 3G9, Canada
E-mail: warren.chan@utoronto.ca
Y. Y. Chen, B. R. Kingston, Prof. W. C. W. Chan
Terrence Donnelly Centre for Cellular and Biomolecular Research
University of Toronto
Toronto, Ontario M5S 3E1, Canada
Prof. W. C. W. Chan
Department of Chemical Engineering and Applied Chemistry
University of Toronto
Toronto, Ontario M5S 3E5, Canada
Prof. W. C. W. Chan
Department of Material Science and Engineering
University of Toronto
Toronto, Ontario M5S 1A1, Canada
Prof. W. C. W. Chan
Department of Chemistry
University of Toronto
Toronto, Ontario M5S 3H6, Canada
The ORCID identification number(s) for the author(s) of this article can be found under https://doi.org/10.1002/admt.202000103.

DOI: 10.1002/admt.202000103

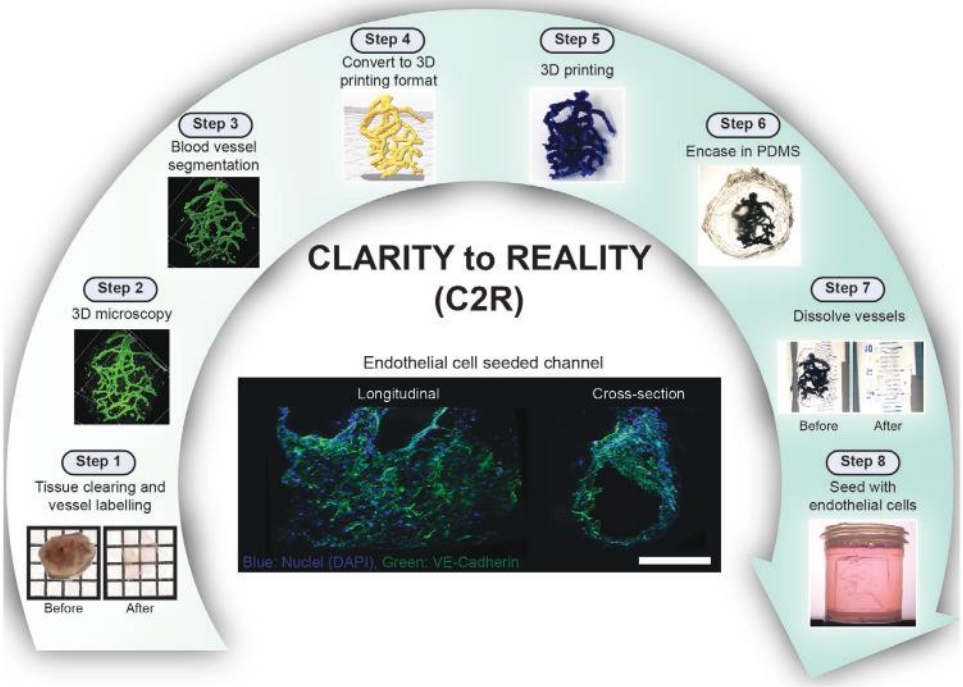

Figure 1. Converting 3D microscopy images of vasculature into a perfusable microfluidic device. The workflow for the CLARITY[22] to REALITY (C2R) process. First, tissues are rendered transparent and blood vessels are labelled (step 1). Next, a 3D microscopic image of the vessel network is acquired (step 2). In step 3 the vessel network is segmented. In step 4 the vessel network is converted to the .stl file format for 3D printing. In step 5 the vessel network is printed with polylactic acid (PLA). In step 6 the printed network is cast in polydimethylsiloxane (PDMS) with inlet and outlet ports. The PLA vessel network is dissolved in step 7 using dichloromethane (DCM). In step 8 the device is coated with collagen and seeded with endothelial cells. The center inset is a 3D microscopy image of endothelial cells coating the walls of a channel inside the device. Scale bar 500 μm.

convert a database of blood vessel images into physical in vitro models of in vivo vasculature for educating and testing drug and nutrient transportation and interaction with endothelial cells.

2. Results and Discussion

The CLARITY-to-REALITY process takes images of blood vessel networks from intact tissues and transcribes them into a perfusable device, as shown in **Figure 1**. The first step is to generate images of blood vessel networks from different tissues. We did this by using tissue clearing and optical microscopy. First, the tissues are cleared using CLARITY,[22] and the blood vessels are fluorescently labeled (Figure 1, step 1). By using tissue clearing and optical imaging we are able to capture micrometer-level details of the vasculature over millimeter depths. This supplies us with highly resolved images that allow us to replicate fine vessel features in a microfluidic device. We labeled the blood vessels of the tissues using anti-VE-Cadherin antibodies in human tissues, and Griffonia Simplicifolia Lectin 1 conjugated to Cy3 dye (GSL-1-Cy3) in mouse tissues.[23] Although this study uses CLARITY to render the tissues transparent, it may not be the optimal technique for all researchers because some proteins will be degraded chemically, and processing and labeling tissues can take weeks. Alternative methods may be used to render tissues transparent for subsequent 3D imaging. The second step is to use light sheet microscopy (Zeiss Lightsheet Z.1 microscope) to image the intact blood vessel networks in 3D. In step 3, we segment the blood vessels using a machine learning-based classification tool called ilastik[24,25] along with pre- and post-processing steps to normalize the fluorescence intensity and remove segmentation artifacts.[26] The result is a segmented, binary image of the blood vessel network. In step 4, we convert this binary image into the stereolithography file (.stl) format, which is suitable for most 3D printers. Only the largest connected vessel network is converted to be 3D printed to enable a single perfusable vessel network. The database of .stl files used in this paper have been made freely available (https://figshare.com/s/f8d884580db2e24728c1).

We then print out the vessel network and construct the physical device. In step 5, we print the vessel network using the Ultimaker 2+ 3D printer with PLA filament. We chose this printer and filament material because they are commercially available and inexpensive. PLA is the most commonly available 3D printing filament material, and fused filament fabrication 3D printers are commonly available and cost as little as $200. In step 6, we cast polydimethylsiloxane (PDMS) around the 3D printed vasculature. Details on casting the device in PDMS are in Figure S1 (Supporting Information). PDMS is a commercially available, easy-to-use polymer that is commonly used in soft lithography to produce microfluidic devices. After curing the PDMS, in step 7 we dissolved the PLA by immersing the device in dichloromethane (DCM) over a period of 24–72 h. This resulted in a 3D microfluidic device that is imprinted with the in vivo vascular geometry (Figure 1, step 7). The PDMS device is gradually deswelled[27] in decreasing concentrations

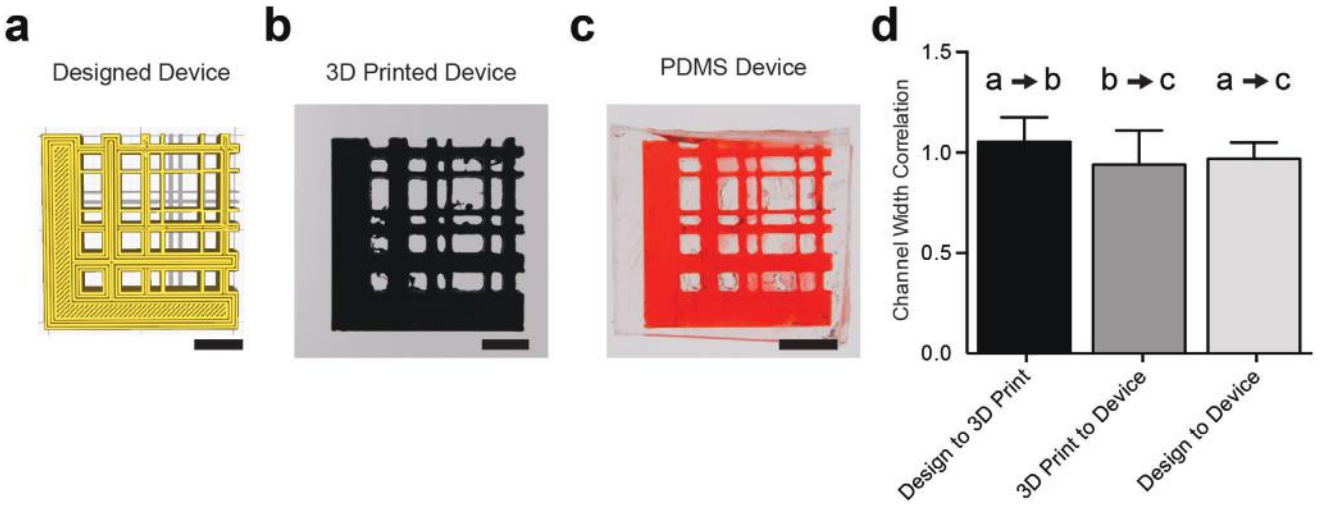

Figure 2. Quantification of information loss through the C2R process. a) A designed grid device with channels ranging from 4 to 500 µm. b) The 3D printed grid device. c) The PDMS grid device perfused with red dye to visualize the channels. d) The channels from the grid device were compared. A value of 1.0 would mean the channel width is exact; larger than 1.0, the channels are larger; smaller than 1.0 the channels are smaller. Between the a) designed device and b) 3D printed device, the correlation is 1.05, standard deviation of 0.21; the b) 3D printed device and c) PDMS device, the correlation is 0.94, standard deviation of 0.17; a) the designed device and c) the PDMS device, the correlation is 0.97, standard deviation of 0.08. Scale bars are 5 mm.

of DCM in ethanol to prevent cracking. The resulting PDMS device is imprinted with the desired vessel network.

The final step is to seed the devices channels with endothelial cells, as shown in Figure 1, step 8. The device is coated with collagen, and then seeded with human umbilical vein endothelial cells (HUVECs). An example of an endothelial cell-coated channel is seen in the center inset of Figure 1. The result of the C2R process is a vascularized microfluidic device with the same vessel architecture as seen in vivo.

The 3D printouts and their corresponding PDMS devices were evaluated at different steps to see if the channel sizes were consistent throughout the C2R process. **Figure 2** and Figure S2 (Supporting Information) show a device that was designed with channels ranging from 4 mm to 500 µm. The channel widths were measured and changes were quantified in Figure 2d and Figure S2 (Supporting Information). Between the designed device (Figure 2a) and the 3D printed device (Figure 2b), the correlation of the channel widths was 1.05. Between the 3D printed device (Figure 2b) and the perfused PDMS device (Figure 2c), the correlation was 0.94. Between the designed device (Figure 2a) and the PDMS device (Figure 2c), the correlation was 0.97. Figure S2 (Supporting Information) shows that channel widths were consistent through the 3D printing process and PDMS casting steps for channels of different widths. On average, the channel widths were consistent throughout the C2R process.

We wanted to ensure that our method was generalizable to different blood vessel architectures found in healthy and diseased tissues. **Figure 3** shows C2R devices created from 3D images of mouse intestinal villi and pancreatic islets. Figure 3a–d and Video S1 (Supporting Information) show the main steps used to create a replicate vascular network of villi in the small intestine. The similarity between the imaged vessels in Figure 3a, and the segmented vessels in Figure 3b or the printed vessels in Figure 3c, was determined to be 0.80 and 0.64, respectively (Figure S3, Supporting Information). The low similarity of the printed vessels is because only the largest connected vessel network is printed. Vessels that are not connected to this network would not be perfused, and are therefore excluded. Analyzing the inset images from Figure 3a–c, the similarity between the imaged vessels and the segmented vessels is 0.98, and the imaged vessels and printed vessels is 0.89 (Figure S3, Supporting Information). The .stl file for the intestines is available in Stl File S1 (Supporting Information). The final villi vessel network is shown in Figure 3e after perfusing it with red dye. Similarly, 3D microscopy images were taken of a pancreatic islet within a cleared mouse pancreas (Figure 3f and Video S2, Supporting Information). The red, spherical region in Figure 3f is the insulin-producing islet microstructure found within the pancreas and is shown by the dashed yellow line in Figure 3g. Figure 3h is the final pancreatic islet device after perfusing it with red dye (Stl File S2, Supporting Information). These examples highlight our ability to replicate healthy vasculature.

We produced devices that recapitulate the complex blood vessel structures observed in solid tumors. These diseased tissues contain dysfunctional vessel networks that are unpredictable and unique to each tumor. In Figure S4a (Supporting Information) we applied C2R to U87MG xenograft glioblastoma tumors (Videos S3 and S4 and Stl Files S3 and S4, Supporting Information). In Figure S5 (Supporting Information) we quantified the diameter of the vessel channels from the device in the top of Figure S4a (Supporting Information). The Pearson correlation between the vessel diameters of the designed vessel network and the actual final device was 0.93. The mean diameter for the designed vessel channels was 877 µm (SD 324 µm) and for the final C2R device was 823 µm (SD 260 µm). In Figure S4b of the Supporting Information (Video S5 and Stl File S5, Supporting Information), we created a C2R device from the blood vessel network of a murine breast tumor model. Figure S4c of the Supporting Information (Video S6 and Stl File S6,

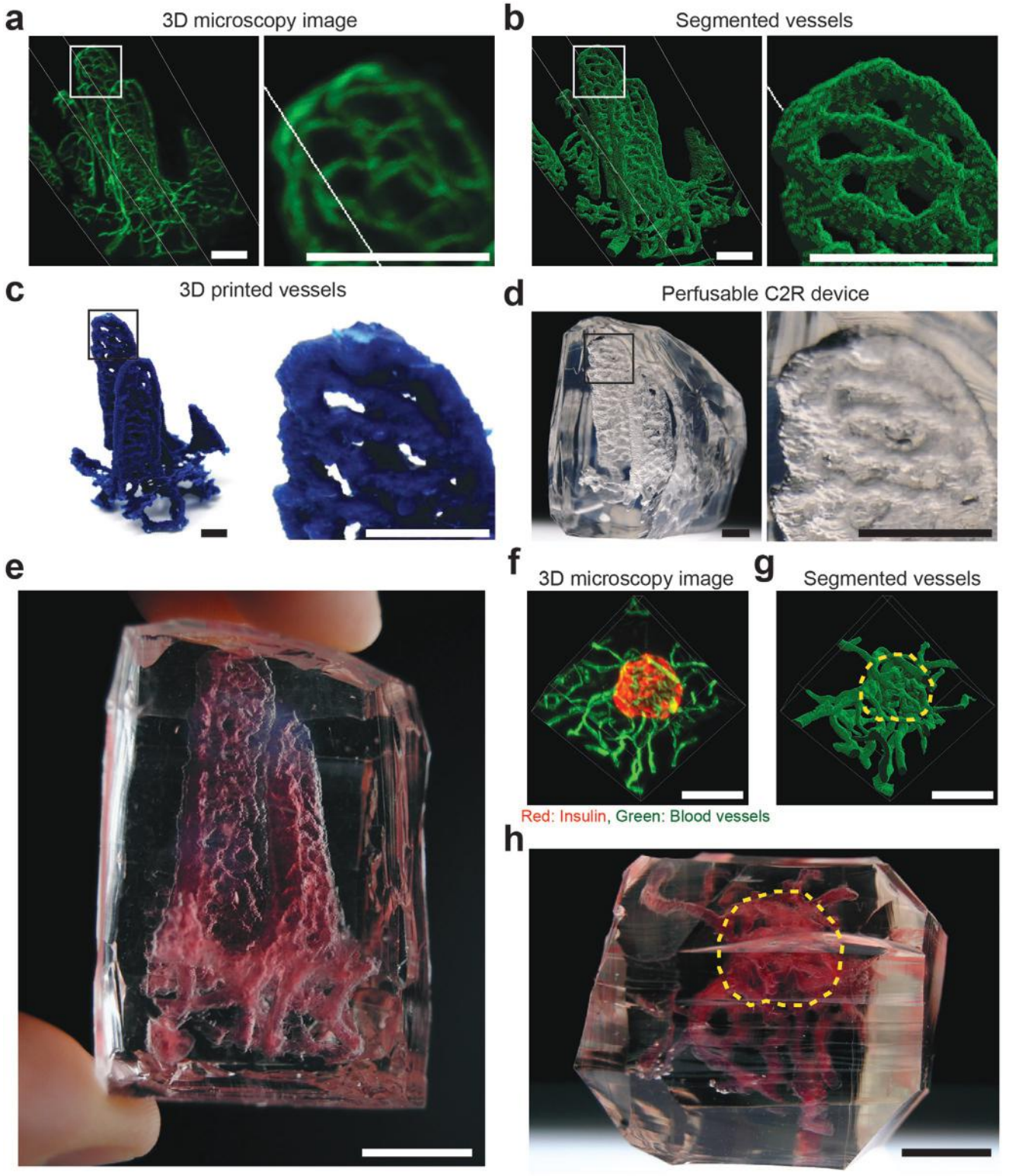

Figure 3. C2R devices recapitulate vessel architecture seen in healthy tissues. a) Blood vessels in villi of the small intestine were imaged with light sheet microscopy, b) the blood vessels were segmented, c) the segmented blood vessels were 3D printed and d) cast in PDMS. e) A C2R device of two villi perfused with red dye. f) A 3D microscopy image of a pancreatic islet and surrounding vasculature. g) The segmented blood vessels from (f) with the islet outlined by the yellow dashed line. h) A C2R device of the pancreatic islet in (f) and (g) perfused with red dye. Scale bars 100 µm in (a), (b), (f) and (g); 5 mm in (c) and (d); 1 cm in (e) and (h).

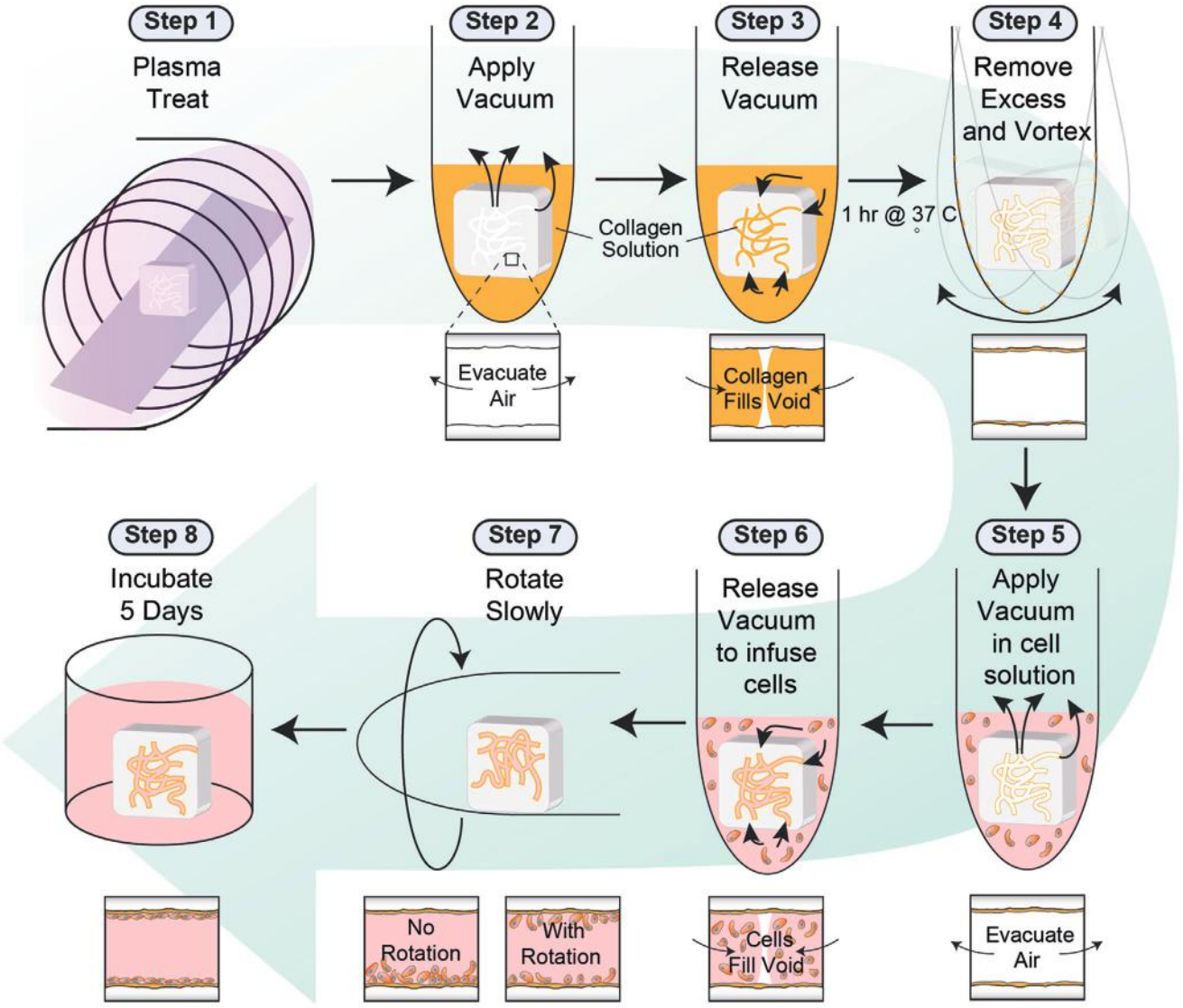

Figure 4. The workflow for seeding C2R devices with endothelial cells. The first step to seed cells is to plasma treat the surfaces of the device. Next, vacuum is applied to remove air from the channels with the device submerged in collagen solution. The vacuum is removed and collagen solution fills the voids of the device. After 1 h at 37 °C the excess collagen is removed leaving a thin layer of collagen coating the channels. Endothelial cells are seeded by applying a vacuum to the device while submerged in media and endothelial cells. The vacuum is released and cells are infused within the vessel network. The device is rotated slowly for 5 h to ensure cells are seeded on all surfaces of the vessels. Endothelial cells are cultured for 5 days to allow them to grow into a monolayer covering the channels of the device.

Supporting Information) is a device of the vessel network of a human ovarian tumor biopsy. This demonstrates the ability of our method to capture and print unique vasculature networks, including those of patient tumor biopsies.

After fabricating PDMS devices we needed to coat the interior walls with endothelial cells to mimic the natural blood vessels. The complex structure of the vessel networks meant that injecting cells into the devices would not result in uniform cell coverage. We developed a new method to seed cells into printed vasculature. The overall method is shown in **Figure 4**. We used human umbilical vein endothelial cells (HUVECs) in our devices, as they are an inexpensive, representative cell type for generating endothelium. As shown in Figure 4 step 1, we first made the interior surfaces hydrophilic by plasma treating the device. The interior walls of the PDMS devices were coated in step 2 by immersing them within a 0.05 mg mL^{-1} collagen solution and applying a vacuum to evacuate the air within the device. When the vacuum is removed in step 3, the collagen solution fills the vessel channels. This ensures complete coverage of the vessel walls with collagen. The device is left in the collagen solution for 1 h at 37 °C. Excess collagen is removed in step 4. The result is a thin layer of collagen coating the vessel channels. The device is now ready for endothelial cell seeding.

To seed the device with cells, HUVECs were cultured and resuspended at 2.5×10^6 cells mL^{-1}. In step 5 the collagen-coated devices are submerged in the cell solution and vacuum is applied, drawing the air out of the device. In step 6 the vacuum is released, causing the cells to rush into the vessel network.

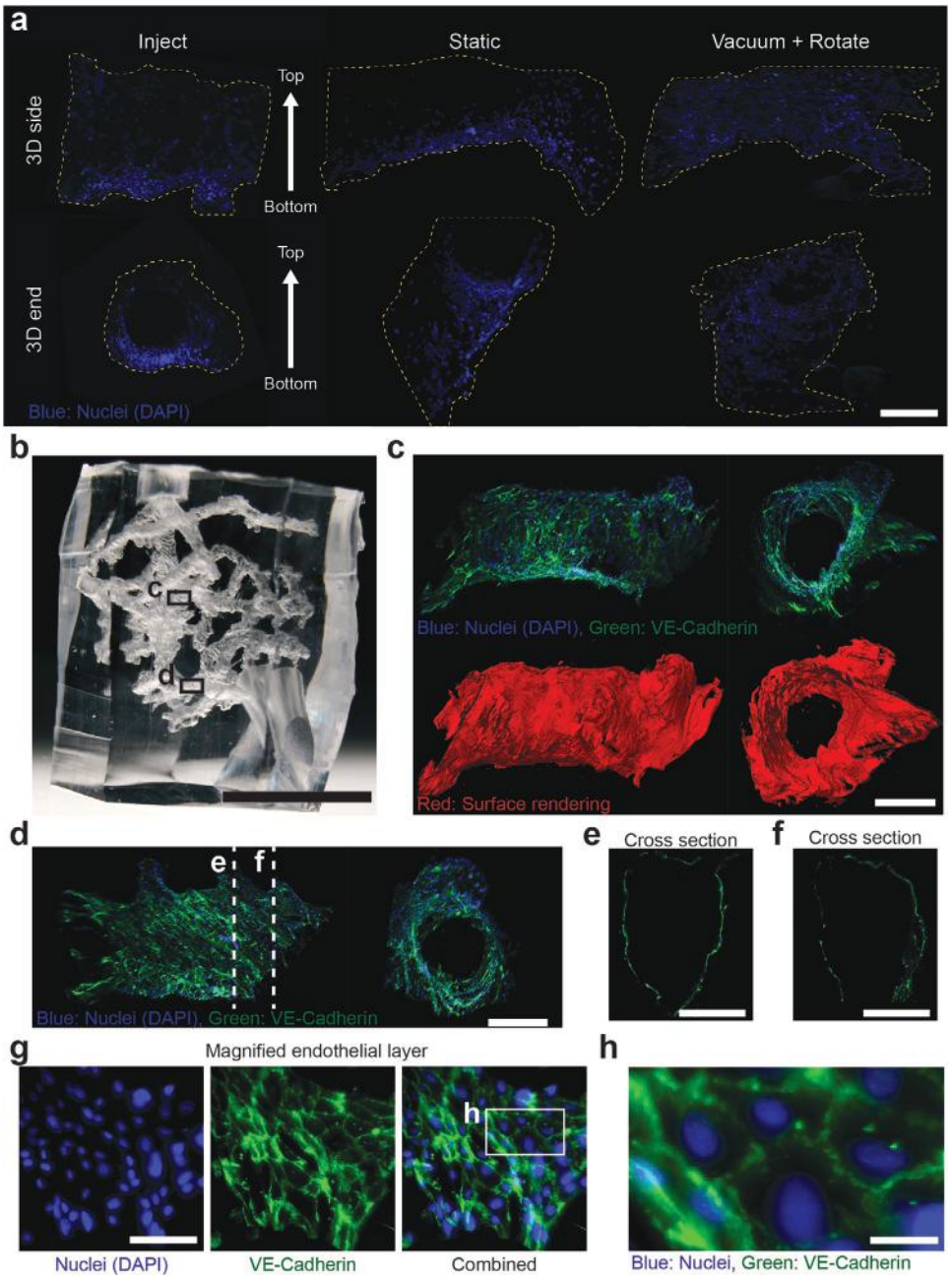

Figure 5. C2R devices lined with endothelial cells. a) 3D images taken by light sheet microscopy show the differences in endothelial cell seeding by a single injection of cells through the inlet, static incubation, or by the vacuum and rotation method. b) Photograph of a C2R PDMS device. c,d) Fluorescent 3D images taken by light sheet microscopy of regions within the device shown in panel (b). e,f) 2D-cross-sections of (d) are shown. g,h) A magnified 3D image of a monolayer of endothelial cells is shown. Scale bar 500 µm in (a) and (c)–(f); 1 cm in (b); 100 µm in (g) and 25 µm in (h).

The excess cell solution is removed and in step 7 the PDMS device is turned sideways and allowed to rotate slowly at 37 °C for 5 h to ensure even cell coverage along the interior walls. The final step is to mature the endothelial cells by incubating them in fresh media for 5 days on a tilting platform. Using alternative methods such as injecting cells into the device or not rotating the device (static) resulted in nonuniform endothelial cell coverage within the device (**Figure 5**a). As shown in Figure 5b–h, the optimized protocol described in Figure 4 resulted in uniform surface coverage of the interior surfaces of the device. Figure 5c,d, and Figure S6 and Video S7 (Supporting Information) show cell coverage in different regions of the C2R device, and positive staining for VE-Cadherin, a protein produced by endothelial cells to form tight junctions between cells. Cross-sections of a vessel within the C2R device are shown in Figure 5e,f with channels around 700 µm in size. A magnified image of the endothelial cell layer is shown in Figure 5g,h, where tight-junctions can be seen as VE-Cadherin staining localized to the cell edges. Through the use of our collagen coating and endothelial cell seeding process, we are

able to achieve uniform cell coverage within the C2R devices to produce vascularized vessels with the architecture of in vivo vasculature.

Using our vascularized PDMS device, we examined the effect of flow patterns on the interactions between a model drug and the endothelial cells of the tumor vessel networks. Successful treatment of tumors will necessitate an understanding of how blood vessel architecture and blood perfusion patterns can change drug interaction with blood vessels of the tumor. We chose a single tumor vasculature network, printed out copies of it, and produced two devices that had the same in-flow point, but different outflow points (**Figure 6**a,b, designs 1 and 2 and Videos S8 and S9, Supporting Information). To determine how changing the outflow points would affect the flow pattern, we first took the two designs and filled them with red dye to ensure that there were no blockages in the channels and that dye could reach everywhere in the device (Figure 6a, 0 min, Figure 6b, 0 min). Next, we perfused blue dye through the two devices, as shown in Figure 6a,b. We observed that in design 1, many regions remained red, since the flow pattern through the device allowed the blue dye to bypass those regions of the vessel network (Figure 6a, 5 min). In design 2, the majority of the device was perfused with blue dye (Figure 6b, 5 min), except for a channel in the upper right region of the device. With these flow patterns in mind, we determined if we could use our devices to examine interactions between endothelial cells and perfused drugs. We printed out two more copies of the same design, produced devices from the printouts, seeded them with endothelial cells as described above, and perfused them with a model drug. For our model drug, we opted to use a carboxyfluorescein-based dye known as carboxyfluorescein diacetate-succinimidylester (CFDA-SE). This dye crosses into the cell membrane and is cleaved by cellular esterases to produce a fluorescent molecule that is cell-impermeable, ensuring cells that are metabolically active become fluorescent. We infused CFDA-SE at 10×10^{-6} M, at flow rates of 500 μL min^{-1} for 5 min in the 2 devices, as shown in Figure 6a,b. The devices were sectioned, fixed, and stained for nuclei (DAPI) and imaged with 3D light sheet microscopy. In Figure 6c we see that the upper right region of the vessel network in design 1 is exposed to the dye and we see green fluorescent signal. In Figure 6d the same upper right region of design 2 has very little green fluorescent signal, indicating dye did not reach this region. In Figure 6e we see that the lower left region of the device did not receive dye in design 1, but Figure 6f shows that this region did receive dye in design 2. Images from an additional region where dye was expected to flow through in both designs are shown in Figure S7 (Supporting Information). We found that regions that underwent red-to-blue dye exchange were positive for CFDA-SE staining because the fluorescent dye was able to flow through these regions of the device. This information suggests that the flow patterns of the same vessel network is determined by the position of the inlet and outlets, and the geometry of the vasculature.

3. Conclusion

We have developed a simple and accessible method to transcribe in vivo vasculature into an in vitro microfluidic device. Using our protocol, we replicated the architecture of blood vessel networks from healthy and diseased tissues in 3D microfluidic devices. We also developed a method to line the vessels of these complex devices with endothelial cells, which can be applied to similar devices. While existing methods such as laser degradation provide beautiful resolution,[19] and other methods using custom 3D printers and bioinks enable the incorporation of different cell types,[14–16] they require expensive or customized equipment that is unavailable for many researchers and educators. Many applications may not require the precise resolution of the laser ablation-based methods, or the cellular complexity of the 3D printing methods. Our channel resolution ranges from 500 μm to 1 cm, which is similar to other 3D printing techniques[21] and is done with off-the-shelf 3D printers and inexpensive PLA filament. The use of an expensive high-resolution 3D printer could improve the resolution of the 3D printed models, and their final PDMS device channels. Currently, many of these advanced printers do not use PLA filament and use resins that may not be soluble in common solvents. Advancements in 3D printing technologies will likely improve the printing quality and resolution with PLA inks, and we may also see the development of new inks and resins that can be used as sacrificial templates. Both of these potential solutions would allow C2R to replicate more detailed vascular structures such as capillaries. The C2R method is useful for experiments requiring a simple, endothelialized device imprinted with vascular networks, or for creating large visual aids for education and outreach. Generally, researchers are limited to using simple channel devices to study endothelial cells under flow. With the C2R method they can now study how changes in flow throughout different areas of a vessel network change drug or cell interactions with endothelial cells. Researchers studying topics such as drug delivery to endothelial cells, or cellular adhesion to endothelial cells by immune or cancer cells, can now do so in vascular networks with flow patterns similar to the in vivo vessel networks. Other potential applications of the C2R workflow may include producing devices of other biological structures, such as lymphatics and neuronal networks. Although this project uses images generated from light sheet microscopy, our technique can be modified for vasculature generated from magnetic resonance imaging (MRI), positron emission tomography (PET), ultrasound, or other imaging technologies. We chose to use tissue clearing and light sheet microscopy because it provides micrometer-level resolution, and was able to capture the vessel features that we wanted to replicate in our microfluidic devices. Other imaging methods could be used to capture vasculature at different scales to manufacture larger, higher-level devices. In this manner, digital databases of vessel networks can be downloaded and used to create in vitro models for studying drug and nutrient interactions with endothelial cells within C2R devices under different flow conditions. Future advancements in 3D printing may allow the creation of higher resolution C2R devices that are closer in size to their source tissues.

4. Experimental Section

Tissues were rendered transparent via the CLARITY process, and then imaged with light sheet microscopy (Zeiss Lightsheet Z.1 microscope)

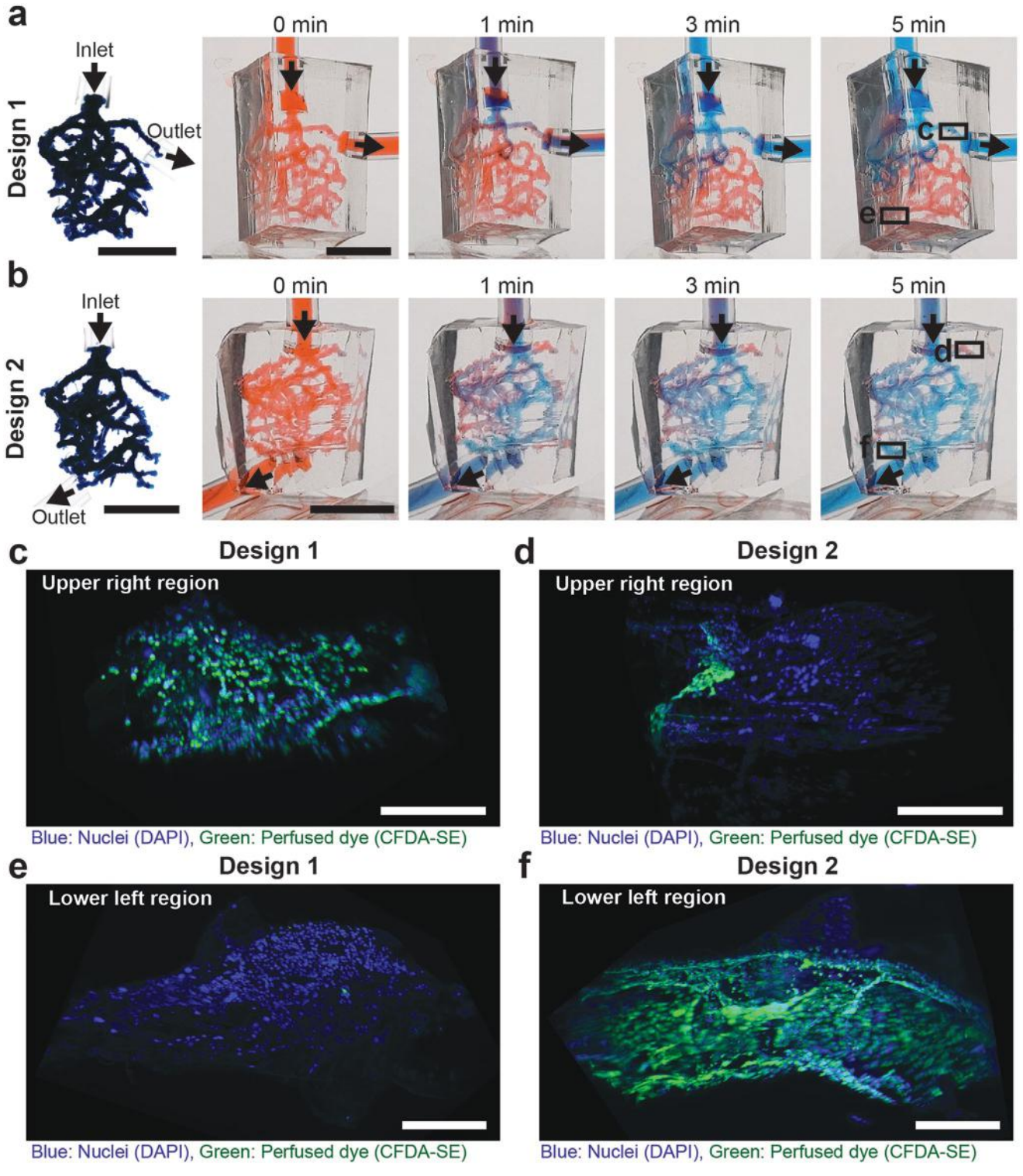

Figure 6. C2R devices show changes in dye distribution based on changes in the perfusion of the vessel network. a,b) Two designs of the same vessel network were created with the inlet ports in the same location, and the outlets in different locations. The devices were filled with red dye to demonstrate that there were no blockages in the channels. Blue dye was perfused through the devices to visualize the flow pattern of the vessel network. New devices of the same designs were seeded with HUVEC cells and were perfused with a fluorescent dye (CDFA-SE). Regions (c)–(f) were imaged using microscopy to detect the presence of the perfused cellular dye. 3D images of the upper right region of the devices is shown in (c) for design 1 and (d) for design 2. 3D images of the lower left region of the devices is shown in (e) for design 1 and (f) for design 2. Scale bar is 1 cm in (a) and (b); 500 μm in (c)–(f).

to obtain a 3D image of their intact blood vessel network. This 3D image of vasculature was converted by the MATLAB script into a 3D-printable stereolithography file that is compatible with most 3D printers. The files were printed out using PLA filament with the Ultimaker 2+, then a 10:1 PDMS:crosslinker mixture was prepared. This mixture was poured around the 3D-printed model, and allowed to cure at 37 °C overnight. Excess PDMS was cut away to expose the inlets/outlets of the 3D-printed model. The 3D-printed model within the PDMS was then dissolved by immersing the entire device in DCM, which would dissolve the PLA filament via the inlets/outlets over the next 24–72 h. The devices were placed in a 50/50 v/v DCM/ethanol solution to deswell for 2 h, then placed in 100% ethanol overnight to remove DCM from within the PDMS. The device was removed from ethanol and dried at 50 °C for 1 day. To seed HUVECs, the interior walls of the devices were plasma treated, then coated with 0.05 mg mL^{-1} collagen solution. Devices were immersed in collagen solution, vacuum was applied to evacuate the air within the channels, then atmosphere was quickly restored which forced the collagen solution into the vessel channels. After incubation at 37 °C for 1 h, the collagen solution was removed and the device was immersed in a HUVEC solution at 2.5×10^6 cells mL^{-1}. Cells were seeded through application and removal of vacuum, then the device was rotated for 5 h, before the device was immersed in endothelial growth media (EGM) and cultured at 37 °C, 5% CO_2 for 5 days. For imaging, devices were sectioned, fixed with 4% formalin, stained for nuclei and VE-Cadherin expression, and imaged with light sheet microscopy. See Appendix (Supporting Information) for more details.

5. Ethical Statement

All experiments involving animals were done in accordance with and approved by the University of Toronto Animal Care Committee. Experimental procedures with human samples were approved by the Research Ethics Board at the University of Toronto (protocol ID 34558). All required guidelines with respect to sample handling and confidentiality were followed.

Supporting Information

Supporting Information is available from the Wiley Online Library or from the author. All .stl files used in this project can also be found at (https://figshare.com/s/f8d884580db2e24728c1).

Acknowledgements

B.R.K. thanks the Natural Sciences and Engineering Research Council of Canada (NSERC), the Royal Bank of Canada (RBC), Borealis AI, the Jennifer Dorrington award, and the Cecil Yip award for student fellowships and scholarships. Y.Y.C. thanks the Natural Sciences and Engineering Research Council of Canada (NSERC), Kristi Piia Callum Memorial Fellowship, and Teresina Florio Memorial Fellowship for funding support. W.C.W.C. acknowledges NSERC Grant 2015-06397; Collaborative Health Research Program Grant CPG-146468; Canadian Institute of Health Research Grants FDN159932 and MOP-1301431; Canadian Research Chairs Program Grant 950-223824; and Canadian Cancer Society Grant 705285-1.

Conflict of Interest

The authors declare no conflict of interest.

Author Contributions

Y.Y.C. and B.R.K. contributed equally to this work. Y.Y.C., B.R.K., and W.C.W.C. designed research; Y.Y.C. and B.R.K. performed research; Y.Y.C. and B.R.K. contributed new reagents/analytic tools; Y.Y.C. and B.R.K. analyzed data; and Y.Y.C., B.R.K. and W.C.W.C. wrote the paper.

Keywords

3D printing, blood vessels, microfluidics, tissue engineering

Received: February 11, 2020
Revised: March 20, 2020
Published online: April 27, 2020

[1] R. Monahan- Earley, A. M. Dvorak, W. C. Aird, *J. Thromb. Haemostasis* **2013**, *11*, 46.
[2] G. Gao, J. H. Lee, J. Jang, D. H. Lee, J.-S. Kong, B. S. Kim, Y.-J. Choi, W. B. Jang, Y. J. Hong, S.-M. Kwon, D.-W. Cho, *Adv. Funct. Mater.* **2017**, *27*, 1700798.
[3] Y. Cheng, F. Zheng, J. Lu, L. Shang, Z. Xie, Y. Zhao, Y. Chen, Z. Gu, *Adv. Mater.* **2014**, *26*, 5184.
[4] Y. Yu, L. Shang, J. Guo, J. Wang, Y. Zhao, *Nat. Protoc.* **2018**, *13*, 2557.
[5] Y. Yu, W. Wei, Y. Wang, C. Xu, Y. Guo, J. Qin, *Adv. Mater.* **2016**, *28*, 6649.
[6] H. Onoe, T. Okitsu, A. Itou, M. Kato-Negishi, R. Gojo, D. Kiriya, K. Sato, S. Miura, S. Iwanaga, K. Kuribayashi-Shigetomi, Y. T. Matsunaga, Y. Shimoyama, S. Takeuchi, *Nat. Mater.* **2013**, *12*, 584.
[7] W. Jia, P. S. Gungorozkerim, Y. S. Zhang, K. Yue, W. Liu, Q. Pi, B. Byambaa, M. R. Dokmeci, S. R. Shin, A. Khademhosseini, Z. Hospital, C. Disease, S. Arabia, *Biomaterials* **2016**, *106*, 58.
[8] A. Tocchio, M. Tamplenizza, F. Martello, I. Gerges, E. Rossi, S. Argentiere, S. Rodighiero, W. Zhao, P. Milani, C. Lenardi, *Biomaterials* **2015**, *45*, 124.
[9] X.-Y. Wang, Z.-H. Jin, B.-W. Gan, S.-W. Lv, M. Xie, W.-H. Huang, *Lab Chip* **2014**, *14*, 2709.
[10] A. P. Golden, J. Tien, *Lab Chip* **2007**, *7*, 720.
[11] W. Wu, A. DeConinck, J. A. Lewis, *Adv. Mater.* **2011**, *23*, H178.
[12] V. K. Lee, D. Y. Kim, H. Ngo, Y. Lee, L. Seo, S.-S. Yoo, P. A. Vincent, G. Dai, *Biomaterials* **2014**, *35*, 8092.
[13] L. E. Bertassoni, M. Cecconi, V. Manoharan, M. Nikkhah, J. Hjortnaes, A. L. Cristino, G. Barabaschi, D. Demarchi, M. R. Dokmeci, Y. Yang, A. Khademhosseini, *Lab Chip* **2014**, *14*, 2202.
[14] D. B. Kolesky, K. A. Homan, M. A. Skylar-Scott, J. A. Lewis, *Proc. Natl. Acad. Sci. USA* **2016**, *113*, 3179.
[15] D. B. Kolesky, R. L. Truby, A. S. Gladman, T. A. Busbee, K. A. Homan, J. A. Lewis, *Adv. Mater.* **2014**, *26*, 3124.
[16] J. S. Miller, K. R. Stevens, M. T. Yang, B. M. Baker, D.-H. T. Nguyen, D. M. Cohen, E. Toro, A. A. Chen, P. A. Galie, X. Yu, R. Chaturvedi, S. N. Bhatia, C. S. Chen, *Nat. Mater.* **2012**, *11*, 768.
[17] M. Hu, A. Dailamy, X. Y. Lei, U. Parekh, D. McDonald, A. Kumar, P. Mali, *Adv. Healthcare Mater.* **2018**, *7*, 1800845.
[18] N. Brandenberg, M. P. Lutolf, *Adv. Mater.* **2016**, *28*, 7450.
[19] K. A. Heintz, M. E. Bregenzer, J. L. Mantle, K. H. Lee, J. L. West, J. H. Slater, *Adv. Healthcare Mater.* **2016**, *5*, 2153.
[20] V. Saggiomo, A. H. Velders, *Adv. Sci.* **2015**, *2*, 1500125.
[21] R. Xie, W. Zheng, L. Guan, Y. Ai, Q. Liang, *Small* **2019**, *16*, 1902838.

[22] K. Chung, J. Wallace, S.-Y. Kim, S. Kalyanasundaram, A. S. Andalman, T. J. Davidson, J. J. Mirzabekov, K. A. Zalocusky, J. Mattis, A. K. Denisin, S. Pak, H. Bernstein, C. Ramakrishnan, L. Grosenick, V. Gradinaru, K. Deisseroth, *Nature* **2013**, *497*, 332.
[23] A. M. Syed, S. Sindhwani, S. Wilhelm, B. R. Kingston, D. S. W. Lee, J. L. Gommerman, W. C. W. Chan, *J. Am. Chem. Soc.* **2017**, *139*, 9961.
[24] S. Berg, D. Kutra, T. Kroeger, C. N. Straehle, B. X. Kausler, C. Haubold, M. Schiegg, J. Ales, T. Beier, M. Rudy, K. Eren, J. I. Cervantes, B. Xu, F. Beuttenmueller, A. Wolny, C. Zhang, U. Koethe, F. A. Hamprecht, A. Kreshuk, *Nat. Methods* **2019**, *16*, 1226.
[25] C. Sommer, C. Straehle, K. Ullrich, F. A. Hamprecht, in *Eighth IEEE Int. Symp. on Biomedical Imaging (ISBI)*, IEEE, Piscataway, NJ **2011**, p. 230.
[26] B. R. Kingston, A. M. Syed, J. Ngai, S. Sindhwani, W. C. W. Chan, *Proc. Natl. Acad. Sci. USA* **2019**, *116*, 14937.
[27] C. V. Rumens, M. A. Ziai, K. E. Belsey, J. C. Batchelor, S. J. Holder, *J. Mater. Chem. C* **2015**, *3*, 10091.

